JOURNAL OF PROPULSION AND POWER
Vol. 14, No. 4, July–August 1998

Vortex Formation and Stability in a Scaled Gas-Core Nuclear Rocket Configuration

L. E. Thode,* M. C. Cline,† and S. D. Howe‡
Los Alamos National Laboratory, Los Alamos, New Mexico 87544

Realistic interplanetary space exploration depends critically upon the development of a high-specific-impulse propulsion system. Previous studies indicate that the specific impulse of an open-cycle gas-core nuclear rocket (OCGCNR) might approach 3000 s. Although the OCGCNR is deceptively simple in concept, it will be difficult to develop in practice because the core is a uranium plasma that must be nearly totally confined. Before constructing a more comprehensive model for this engine, there is a requirement to understand the limits of present full-scale simulation models and recent scaled experiments. In this scoping study we have used a two-dimensional, axisymmetric, finite difference code to investigate the formation and stability of a recirculation region observed in a scaled experiment. It has been proposed that such a recirculation region, or vortex, might provide improved confinement of the uranium fuel. Our simulation results indicate that a more comprehensive model must treat the rocket nozzle in a self-consistent fashion to properly calculate the confinement of the uranium plasma. Under conditions that lead to vortex formation, the position of the vortex depends upon the inlet geometry and injection velocity, the nozzle position and subsonic convergence angle, the base-bleed injection rate, and turbulence. With a large base-bleed injection rate, a vortex forms but is then swept away through the nozzle, a result that resolves an inconsistency between a full-scale engine simulation model and recent scaled experiments.

Introduction

WITHIN the next 30 years a human crew will likely brave the isolation, radiation, and the lack of gravity to walk on and explore Mars. Nevertheless, because the mission distance and duration will be hundreds of times greater than the lunar mission, a human crew will face far greater obstacles and a higher risk than those experienced during the Apollo program. A single solution to many of these obstacles is to dramatically decrease the mission duration by developing a high-performance propulsion system.

Several studies[1–3] over the past decade have identified the difficulties of sending manned missions beyond the moon. Most prominent of these difficulties are the radiation levels of nearly a REM per week from galactic cosmic rays and the substantial decalcification of bone that occurs in a zero-gravity environment. In addition, psychological problems associated with living in confined quarters for long periods of time have been indicated by incidents onboard the Russian space station, MIR. The effects of all of these threats can be mitigated substantially by reducing the total mission time to about 9 months. To reduce mission time and, at the same time, maintain a reasonable mass fraction for the initial mass in low earth orbit of the ship, a high-thrust propulsion system with a specific impulse exceeding 2000 s will be required.

The best chemical propulsion system developed so far has a specific impulse of about 460 s, limited by the amount of specific energy that can be generated by the propellants. For a solid-core nuclear rocket the maximum specific impulse is about 1000 s, limited by the solid-core temperature. For the open-cycle gas-core nuclear rocket (OCGCNR) the specific impulse might approach 3000 s, limited by the wall heat flux. Because the core is actually a plasma, the high specific impulse associated with the OCGCNR is simply a consequence of the high core temperature.

The combined potential of high thrust and high specific impulse offered by the OCGCNR makes it an excellent candidate for an interplanetary space-propulsion system. Although the OCGCNR is deceptively simple in concept, it will be difficult to develop in practice because the core is a uranium plasma that must be almost totally confined.

There are a number of possible configurations for an OCGCNR. In the present paper we only consider the most basic axisymmetric configuration. An annular hydrogen stream (the propellant) is envisioned to hydrodynamically confine a near-critical fissioning uranium plasma (the fuel). The energy liberated during the fission process is ultimately radiatively coupled to the hydrogen as it passes around the confined uranium fuel and out through the nozzle.

The most comprehensive computational OCGCNR model has been developed by Poston and Kammash.[4] The Poston–Kammash (PK) model couples hydrodynamics with neutron transport and radiation diffusion in an axisymmetric configuration. Using this model an extensive study of the OCGCNR was performed. The study confirmed that the OCGCNR is capable of high thrust at high specific impulse. From a practical viewpoint the maximum wall heat flux limited the specific impulse to the range of 2000–3000 s. Despite these encouraging results the study indicated that the uranium plasma containment is very strongly and negatively affected by the rocket acceleration. On the other hand, the PK model does not calculate the nozzle in a self-consistent fashion. Moreover, it is conceivable that an improved model including a self-consistent treatment of the nozzle may not exhibit the same sensitivity to rocket acceleration.

Within the same time frame, a scaled cold-flow hydrodynamic experiment was performed by Sforza et al. (SR).[5] The SR experiment used air to simulate the hydrogen propellant and investigated the formation and control of a recirculation region using a base-injection technique. The experiment was an initial demonstration for an alternate OCGCNR operational

Presented as Paper 97-2955 at the AIAA/ASME/SAE/ASEE 33rd Joint Propulsion Conference, Seattle, WA, July 8, 1997; received Oct. 9, 1997; revision received March 5, 1998; accepted for publication March 7, 1998.

*Laboratory Fellow, Applied Theoretical and Computational Division.

†Technical Staff Member, Theoretical Division, Group T-3. Member AIAA.

‡Technical Staff Member, Applied Theoretical and Computational Division. Member AIAA.

approach. The scenario for an OCGCNR is to establish a recirculation region with the hydrogen propellant and then inject uranium fuel from the base region into the established recirculation region. When the fuel replaces the propellant in the recirculation region, fuel injection ceases and propellant injection is again initiated from the base region. The entire process is repeated once the fuel has been depleted below some specified level.

It is possible that the formation of a recirculation region might improve the uranium plasma containment in the presence of rocket acceleration, even in the basic axisymmetric configuration. So, in an attempt to better understand such a recirculation region, we have performed a scoping study investigating the vortex formation and evolution in this SR experimental configuration.

The fundamental reason for the development of an improved OCGCNR model is to investigate more realistic configurations, all of which are three-dimensional in nature. Thus, in addition to gaining a qualitative understanding of the experiment, the scoping study was intended to determine what limitations exist within the present axisymmetric PK model. For example, with the PK model, there is no indication of the formation of a recirculation region in a full-scale engine configuration. Given this result, there are two possible problems: 1) The computational model is not sufficiently accurate or 2) the physical regime of the SR experiment is not representative of a full-scale engine. For example, in a full-scale engine, the injection velocity is about two orders of magnitude lower than in the SR experiment. The hydrogen injection velocity is set by radiation-absorption considerations, not vortex formation. On the other hand, the Reynolds numbers for a full-scale configuration and the scaled SR experiment are similar, which would indicate a similar flow pattern in the absence of the rocket acceleration. Yet, with the much higher injection velocity, the SR experiment demonstrates the formation and control of a recirculation region.

Given these facts there appears to be an inconsistency with respect to the formation and dimension of a recirculation region in a full-scale OCGCNR engine. At first this inconsistency was thought to be entirely associated with numerical limitations, limitations that needed to be understood before proceeding with the development of an improved simulation model. In the present study numerical limitations associated with mesh size and artificial viscosity have been investigated. To summarize, although the injection velocity and nozzle both prove to be important, we find there is no inconsistency between the full-scale engine model and the scaled SR experiment. Rather, the presence or absence of a vortex depends upon the base-bleed injection rate.

Gas-Core Nuclear Rocket Configuration

As stated previously, there are several possible configurations for an OCGCNR. Nevertheless, this study is limited to the basic OCGCNR configuration depicted in Fig. 1 because the PK model and the SR experiment considered only this basic axisymmetric configuration. The outer wall is actually a pressure vessel surrounded by a moderator. Inside the pressure vessel, hydrogen is injected through an annular inlet region, indicted by inlet flow in the figure. Initially, the hydrogen flow generates a recirculation region or vortex as a result of shear flow on the inner surface of the annulus. Once the vortex is formed, uranium is injected and contained by the vortex and a base injection flow is used to control the downstream position of the vortex.[5]

The vortex region must be determined by the geometry, not by the injection velocity, to allow the uranium plasma to approach critical. Moreover, the neutron range is large compared with the size of the vortex. Thus, a moderator external to the pressure vessel is required to reflect neutrons back into the confined uranium plasma. As the uranium plasma fissions, the fission fragment kinetic energy is converted into a nonthermal

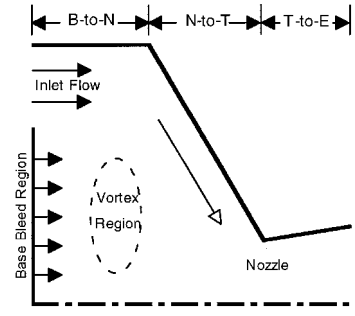

Fig. 1 Basic axisymmetric gas-core nuclear rocket configuration considered in the scoping study.

distribution of electrons. Thus, the fission fragments remain confined to the vortex region. Ultimately, the energy transfer between the uranium plasma and the hydrogen propellant is primarily through radiation. After flowing around the vortex, the high-temperature hydrogen propellant flows out through the nozzle.

There are a large number of fundamental issues and very complex tradeoffs associated with an OCGCNR; but one fundamental issue is the confinement of the uranium plasma under rocket acceleration.[4] Moreover, the uranium-confinement issue cannot be considered without understanding some of the constraints of the overall system. For example, even for a fixed inlet propellant mass flow rate, there is a tradeoff between the injection velocity, injection density, and the area of the annulus. Assume for the moment that the formulation of a recirculation region does indeed provide improved containment of the uranium plasma. Given this assumption the hydrogen injection velocity cannot just be chosen to optimize the vortex, because the efficiency of radiation absorption by the hydrogen propellant depends strongly upon the injection velocity.

Scaled Hydrodynamic Experiment

A scaled hydrodynamic experiment has been constructed and operated by Sforza et al.[5] The experimental chamber geometry is similar to the axisymmetric configuration depicted in Fig. 1. At the inlet, the radius of the porous base plate, through which base injection occurs, is 0.137 m. The radius of the outer wall is 0.194 m. The chamber wall remains at the inlet wall radius for an axial distance of 0.575 m, at which point the wall begins to converge at a 45-deg angle to form the nozzle. The nozzle throat radius is 0.0381 m and is located at an axial distance of 0.725 m from the porous base plate. The transition curves in the nozzle are smooth. However, there is an abrupt transition beyond the throat to atmospheric pressure. The inlet pressure is 202 kPa, which leads to an injection velocity of 15.25 m/s. Except near the walls the injection velocity is nearly uniform across the annular inlet region. The working fluid for the experiment is air. For this configuration the formation of a large recirculation region was demonstrated. In addition, the control of the position of the recirculation region, with base injection through the porous base plate, was demonstrated.

Computational Issues

In this section we describe the code used for the scoping study, provide a summary of the simulations, outline a number of mesh issues, and then provide examples of the impact of artificial viscosity on vortex formation and evolution.

Code Description

We have used the VNAP2 code because of the presence of the nozzle in the experiment.[6] The VNAP2 code solves the single-fluid, two-dimensional, time-dependent, compressible Navier–Stokes equations. The fluid is assumed to be a perfect gas. There are options for inviscid, laminar, and turbulent flow under steady or unsteady conditions. Problems can be solved

Table 1 Summary of the simulations performed in the scoping study

Parameter/model	Baseline case	Variation about baseline
Wall radius	0.194 m	None
Inlet base radius	0.137 m	None
Nozzle throat radius	0.0381 m	0.0098, 0.0138, 0.0169, 0.0239, 0.0293, 0.0338
Inlet base to nozzle inlet length	0.575 m	0.119, 0.199, 0.302, 0.469
Nozzle inlet to throat length	0.154 m	0.30
Throat to nozzle exit length	0.0636 m	None
Nozzle divergence angle	5 deg	1, 10, 15
Mesh size, vortex region	0.35 cm × 0.35 cm	0.75 × 0.75, 1.0 × 1.0
Artificial viscosity coefficient	0.5	0.0, 0.25, 1.0, 3.0, 5.0
Artificial viscosity region	Vortex region	To nozzle, entire mesh
Inlet velocity	15.25 m/s	1.15, 2.0, 3.0, 6.0, 9.0, 12.0
Inlet velocity profile	Experimental	Uniform
Base injection velocity	0.0 m/s	0.31, 0.61, 0.92, 1.53, 4.58
Flow model	Turbulent	Inviscid
Inlet turbulent kinetic energy	1% flow energy	5%, 10%
Turbulence seed region	Inlet	Along streamline, entire mesh
Inlet pressure	202.7 kPa	None
Inlet temperature	300 K	None
Inlet density	2.45 kg/m^3	None

Note: The baseline case corresponds to the scaled SR experimental configuration. Each variation is a separate simulation, except the inlet velocity and nozzle throat radius are modified in one-to-one correspondence to ensure consistent mass flow through the choked nozzle.

in either a Cartesian or cylindrical coordinate system. The grid is nonuniform with body-fitted coordinates in the radial direction. An unsplit MacCormack scheme is used to solve the finite difference equations. Artificial viscosity can be used to control algorithm stability. Typical problems that can be solved by VNAP2 are nozzles, inlets, jet-powered afterbodies, airfoils, and freejet expansions.

The VNAP2 code was integrated into a C++ environment that uses a fragment class to standardize input, output, restart, and graphics. The integrated code was converted to run on workstations and reconfigured with a large number of new diagnostics. All of the simulations were run on an HP 9000/735 workstation in double precision. For this problem, the computational power of this workstation is marginal, particularly for the fine-zone simulations that are 10–40 h in length.

Simulation Summary

Table 1 presents a summary of parameter and model variations. All of the simulations are time dependent. The initial conditions were obtained from a one-dimensional isentropic flow calculation. In a few cases the initial conditions include a seed vortex imposed upon the one-dimensional isentropic flow. The baseline case corresponds to the scaled experimental geometry. In Fig. 1 the inlet base to nozzle inlet length is indicted by B-to-N, the nozzle inlet to throat length is indicated by N-to-T, and the throat to nozzle exit length is indicated by T-to-E.

For the most part, each variation represents a separate simulation. However, the nozzle throat dimension was modified in one-to-one correspondence with the injection velocity, keeping the inlet pressure, temperature, and density fixed. In addition, the throat dimension was modified when base-bleed flow was included in the simulation. For all cases the simulations were designed using a one-dimensional isentropic flow model. In this paper all parameters should be assumed to be that of the baseline case unless otherwise specified.

For the scoping study the geometry was varied significantly about the baseline, including variations in both the vortex and nozzle regions. Three basic mesh sizes within the vortex region were considered. Because VNAP2 generates a mesh that conforms with the nozzle, the corresponding radial mesh size is smaller in the nozzle region. An extensive number of simulations were performed to investigate the impact of artificial viscosity on both the formation and evolution of the vortex.

Both turbulent and inviscid flow models were utilized. Turbulent calculations were only performed for the baseline geometry. A number of techniques were used to seed the turbulence model and the inlet turbulent kinetic energy was varied from 1 to 10% of the inlet kinetic energy. Although the baseline simulation uses the turbulent flow model, most of the simulations use an inviscid flow model because the turbulent model requires a 2-to-3-factor longer run time.

Mesh Size

The mesh size is a complicated issue. Ideally, one would continue to refine the mesh until the solution became mesh independent. Of course, small-scale features continue to change as the mesh is refined, but the large-scale features do often become mesh independent. In the present problem we are interested in the large-scale features of the position, size, and rotation velocity of the vortex. In this sense we have been able to refine the mesh sufficiently when the inlet injection velocity exceeds 3 m/s for the SR experiment. With an injection velocity below 3 m/s, however, the mesh may not be sufficiently refined. For example, we know at least three mesh points are needed to represent a vortex. With respect to a simulation, if the initial vortex size is determined by the injection velocity and the mesh size is too large, then no vortex will form.

There are two regions that must be treated with some care: 1) The region below the inlet injection annulus and 2) the nozzle throat. In the simulations we have been able to vary the mesh size by about a factor of 3. For the baseline experimental configuration the maximum number of cells was 210 in the axial direction and 55 in the radial direction. The mesh is typically nonuniform with the smallest cells located in the nozzle throat region.

Artificial Viscosity

Artificial viscosity is typically used to stabilize an explicit algorithm in the presence of strong shocks. In the SR experimental configuration we did not expect strong shocks and did not use artificial viscosity in the initial simulations. Apart from the experiment, in the scoping study we did allow variations in the geometry. In some cases there are weak shocks formed in the nozzle when the ratio of the injection inlet radius to nozzle throat radius is very large.

As expected, artificial viscosity was not required to observe the formation of the vortex at high inlet injection velocity. However, we were interested in understanding the long-term stability of the vortex, not just the formation. With the longer simulation times, algorithm stability became a problem in the low-speed vortical flow region. As a result, it was necessary to use some artificial viscosity in most of the simulations, be-

cause evolution to quasi-steady-state flow takes a much longer time than required to form the initial vortex.

Artificial viscosity can have a major impact on vortex formation and evolution. The extent of the impact of artificial viscosity is both problem and configuration dependent. The entire subject of artificial viscosity, including solution accuracy, is somewhat subjective. In the SR experimental configuration we observe a strong sensitivity with respect to the fluid injection velocity. At low-velocity injection, less than 1 m/s, artificial viscosity can prevent the formation of a vortex in coarse-zone simulations. At high-velocity injection, above 3 m/s, artificial viscosity can change the position and vorticity of the vortex.

In VNAP2, artificial viscosity can be applied over a specified domain. Given this option, two fundamental issues arise for any simulation: 1) The domain over which the artificial viscosity will be applied and 2) the level of artificial viscosity that can be tolerated in that domain without significantly changing the physics. Referring to Table 1, we studied the impact of artificial viscosity in three regions: 1) The vortex region, 2) the mesh from the base-to-nozzle, and 3) the entire mesh. In each case the magnitude of the applied artificial viscosity was changed by over an order of magnitude.

Impact of Artificial Viscosity on Nozzle Flow

Initially, we added artificial viscosity to the entire OCGCNR configuration including the nozzle. As an example, in Fig. 2 the axial flow velocity is shown as a function of axial position along the configuration centerline. The time is early in the simulation, before the vortex has fully developed. The profile of the inlet velocity is uniform, rather than the experimental profile, and the flow model is inviscid. Without artificial viscosity the rotation region is well defined (negative velocity region in the lower left corner of the figure) and the entire velocity curve is smooth. With artificial viscosity over the entire mesh the rotation velocity has been significantly reduced, the vortex is not as well defined, and the velocity shows unacceptable spiky behavior in the nozzle. From additional simulations we find the spiky behavior seen in Fig. 2 can be attributed to the use of too much artificial viscosity (too large a time step) in the nozzle. In fact, we found artificial viscosity is not required in the nozzle. Thus, artificial viscosity is not used in the nozzle region in any of the scoping simulations.

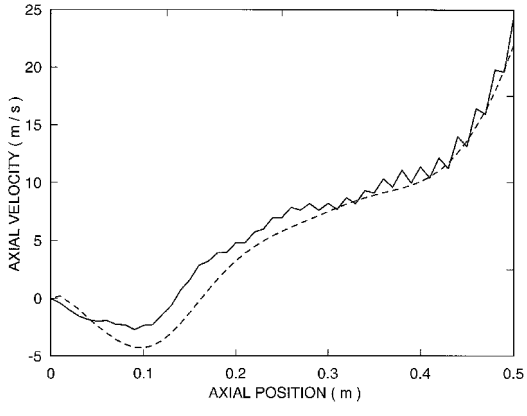

Fig. 2 Axial flow velocity as a function of axial position along the centerline: – – –, without artificial viscosity; ——, with artificial viscosity.

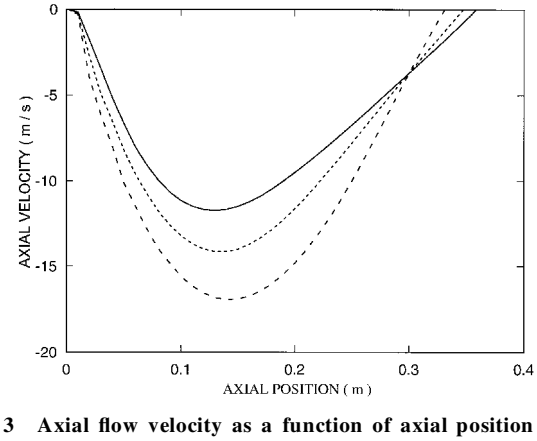

Fig. 3 Axial flow velocity as a function of axial position along the centerline for three different levels of artificial viscosity: – – –, no artificial viscosity; ---, artificial viscosity needed for algorithm stability; ——, high level of artificial viscosity.

Impact of Artificial Viscosity on Vortex Position and Vorticity

In Fig. 3 the axial velocity is shown as a function of axial position along the centerline for three levels of artificial viscosity. The profile of the inlet velocity is uniform, rather than the experimental profile, and the flow model is inviscid. The three artificial viscosity levels are 1) zero, 2) the level needed for algorithm stability (coefficient of 0.5), and 3) a large level to accentuate the impact on the vortex (coefficient of 5.0). No artificial viscosity is applied beyond the axial point where the configuration begins to converge to form the nozzle. In Fig. 3, the largest negative rotation velocity is associated with zero artificial viscosity. As the level of artificial viscosity is increased, the maximum rotation velocity decreases, the point of maximum rotation velocity moves upstream, and the stagnation point moves downstream. In the scoping study we used an artificial viscosity coefficient of 0.5.

Impact of Artificial Viscosity on Vortex Formation

At low-velocity injection, too large a mesh size can prevent the formation of a vortex. Given that the mesh size is sufficient to resolve the initial vortex, artificial viscosity can still prevent the formation of the vortex. This effect is illustrated in Figs.

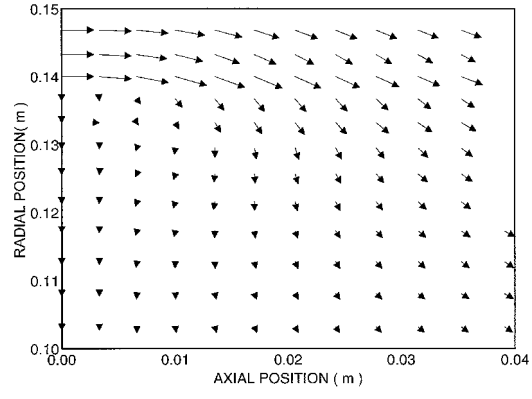

Fig. 4 Vector plot of the velocity field showing the absence of a vortex because of the presence of artificial viscosity.

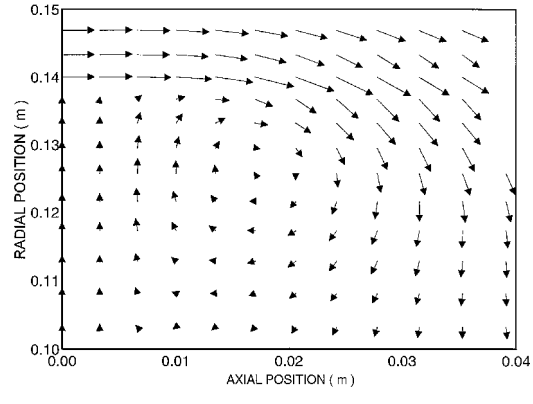

Fig. 5 Vector plot of the velocity field showing the presence of a vortex because of the lack of artificial viscosity.

4 and 5. Both simulations have identical fine-mesh sizes and an injection velocity of 1.15 m/s in the SR experimental configuration. The profile of the inlet velocity is uniform, rather than the experimental profile, and the flow model is inviscid. The only difference between the simulations is the domain over which the artificial viscosity is applied.

In Fig. 4 no evidence of vortex formation is present. The flow simply turns the corner and proceeds toward the axis. In this case, artificial viscosity was applied in the base-to-nozzle region, across the entire radial dimension. In this region, the artificial viscosity was sufficiently large to reduce the local effective Reynolds number to about 1×10^1.

In Fig. 5 a small vortex is clearly present. The vortex is not fully developed but will continue to grow with time. In this simulation the artificial viscosity has been applied only to the region below the injection region, the low-speed vortical region. The local effective Reynolds number has been increased to about 5×10^2 in the region of large shear flow. In the scoping study artificial viscosity was typically only applied in the low-speed vortical region.

Scoping Study Results

In this section we provide the basic results of the scoping study. The formation and evolution the vortex is investigated as a function of the base-bleed injection flow, nozzle position and shape, inlet injection velocity, and turbulence.

Base Injection Flow

Once a vortex is formed, base injection is envisioned to control the downstream position of the vortex. A series of simulations were performed using the experimental configuration. The profile of the inlet velocity is uniform and the flow model is inviscid. In this series, the base injection is uniform across the base. The results are indicated in Fig. 6, where the initial and final downstream position of the vortex is shown as a function of base-bleed ratio. Typically, the vortex grows until limited by geometry and then evolves to slightly farther downstream position. For the SR experimental configuration, the base-bleed ratio is simply the ratio of the injection velocity in the base region to the injection velocity in the annular region assuming the same fluid density in both regions.

At a low base-bleed ratio, indicated by stable vortex in Fig. 6, the simulations are in qualitative agreement with the SR experiment. This result supports the premise that the vortex could be actively controlled using a combination of base injection and inlet injection. On the other hand, at a high base-bleed ratio, indicated by unstable vortex in Fig. 6, the vortex is transient: A vortex initially forms because the annular injection velocity is larger than the base-bleed injection velocity, but then the vortex is swept away through the nozzle by the base-bleed flow. Consequently, in steady state there is no vortex present with a large base-bleed ratio, consistent with the results of the full-scale PK simulation model. This means that the full-scale engine model and SR experiment are not inconsistent but are in different flow regimes.

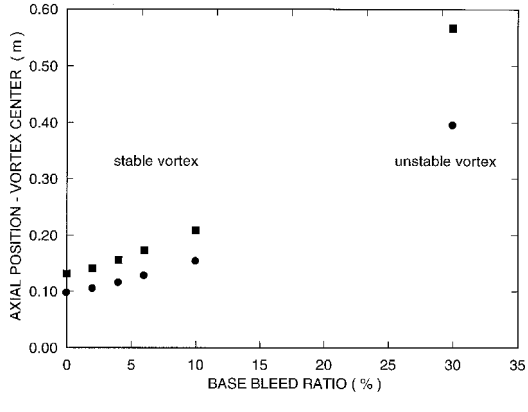

Fig. 6 Axial position of the center of the vortex as a function of the base-bleed ratio. The SR experiment operates in the stable regime whereas the baseline gas-core design calculated from the PK model operates in the unstable regime: ●, initial and ■, downstream position of the vortex.

Nozzle Position

In the SR experiment the distance between the base plate and the nozzle position is large compared to the axial dimension of the vortex. Here, we define the nozzle position as the axial point at which the radial wall begins to converge. Under these conditions we would not expect the vortex formation or evolution to depend strongly upon the nozzle position. From an engine mass standpoint, however, there is a clear disadvantage to the extended distance between the vortex and the nozzle position. Thus, how the nozzle position might impact vortex formation is an important issue.

Given the engine mass issue, we have investigated the impact of nozzle position on the formation and strength of the vortex. In all simulations the injection velocity is uniform across the annular region. Artificial viscosity is applied between the base plate and the nozzle position over the entire radial extent. The flow model is inviscid.

The results of a series of simulations are summarized in Figs. 7 and 8. In these figures, the nozzle position is given in terms of the base-plate radius, which is 0.137 m. As expected, once the nozzle position exceeds about three times the base-plate radius, the vortex position is weakly dependent upon the nozzle position. However, as the nozzle position is decreased, the vortex axial and radial position decrease. When the nozzle position approaches the base-plate radius, the rate of change in the axial position of the vortex begins to slow because the vortex is being pushed against the base plate. Still, the radial vortex position continues to decrease.

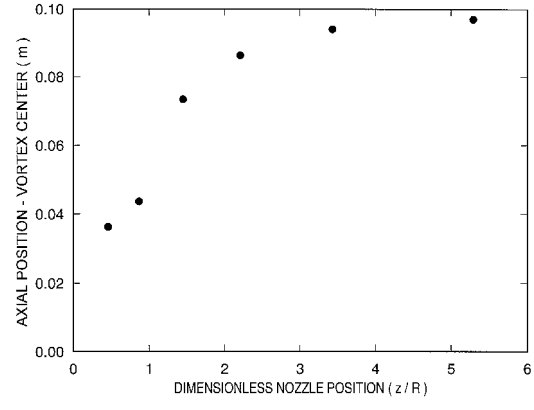

Fig. 7 Axial position of the center of the vortex as a function of nozzle position relative to the base-plate radius.

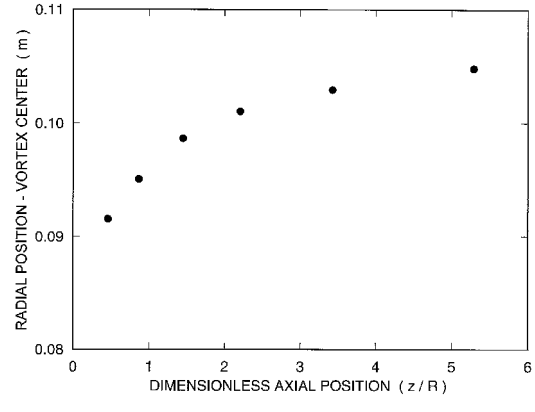

Fig. 8 Radial position of the center of the vortex as a function of nozzle position relative to the base-plate radius.

It is not clear what the optimal nozzle position will be in a full-scale OCGCNR. From these results, however, it is clear that the nozzle must be included in the simulation to correctly understand vortex formation and stability. Because it is conceivable that the formation of a vortex region might improve uranium containment in the presence of rocket acceleration, we infer that a self-consistent treatment of the nozzle would impact the uranium loss rate. To our knowledge all past computational models of the OCGCNR have not calculated the nozzle in a self-consistent fashion. As a result, with respect to the uranium loss rate, previous estimates should be considered suspect.

In addition to the previous series of simulations on nozzle position, we have investigated the impact of vortex formation and stability as a function of the nozzle subsonic convergence angle and nozzle supersonic expansion angle. Again, all of the simulations were performed for the basic SR experimental configuration. As the nozzle convergence angle is decreased, the nozzle becomes longer and the vortex moves downstream. In contrast, the nozzle expansion angle has a minimal impact on the vortex position. Clearly, as the nozzle position is decreased, the impact of the nozzle convergence angle will become more important. Again, this points to the conclusion that a self-consistent treatment of the entire nozzle must be incorporated into a comprehensive OCGCNR simulation model.

Inlet Injection Velocity

An important feature of the recirculation region is the vortex size. If a vortex is to provide useful confinement for the uranium plasma, the vortex size must be set by the geometry. If the vortex becomes smaller with injection velocity, then the uranium criticality will be degraded.

A series of coarse- and fine-zone simulations were performed to investigate the vortex size as a function of injection velocity. In each simulation the nozzle position and subsonic convergence angle are the same. However, the nozzle throat is changed in each case to match the modified inlet mass flow. Except for nozzle throat modifications the simulations are for the baseline experimental geometry.

The inlet flow is injected uniformly across the annular inlet region. A small amount of artificial viscosity was applied over the vortical region to control algorithm stability, but there is no artificial viscosity used in the inlet region. In all simulations the local effective Reynolds number (includes artificial viscosity) exceeded 5×10^2.

In Fig. 9 the axial vortex position, which is an indication of the vortex size, is shown as a function of the inlet injection velocity from 1.15 to 15.25 m/s, we have not attempted any simulations with an inlet injection velocity below 1.15 m/s because of run-time limitations. With a coarse mesh a vortex forms and evolves to a quasi-steady-state condition. Even with a coarse mesh the required run times are quite long to reach a steady-state condition. For the coarse-mesh simulations, the size of the vortex is slightly smaller with lower injection velocity. However, there is no significant indication that the size of the vortex is strongly dependent upon the injection velocity.

Between an inlet injection velocity of 1.15 and 3 m/s, we observe no vortex formation with a coarse mesh when the initial condition is given by a one-dimensional isentropic flow solution. In this case, it is possible to provide an initial condition that contains a seed vortex. With this modified initial condition the seed vortex evolves in time, it moves downstream and continues to increase in size. The coarse-mesh solution at 1.15 m/s injection velocity was achieved using a seed vortex initial condition.

At the lower injection velocities, we did not run any of the fine-mesh simulations long enough to determine if the quasi-steady-state dimension of the vortex is about the same as the coarse-mesh simulations. However, at high-injection velocity, we see no real indication that the coarse- and fine-mesh simulations disagree. In fact, at 15.25-m/s injection velocity, the difference in vortex dimension is not all that dissimilar between the coarse and fine mesh.

All of the fine-mesh simulations were run to about the same physical time. The point of including the fine-mesh results is to demonstrate the evolution rate of a vortex. As the inlet injection velocity decreases, the rate of evolution slows. This effect is particularly true below an injection velocity of 3 m/s, where the size of the initial vortex begins to drop significantly. On the whole, this dependence is not a surprising result, because for a fixed geometry the flow velocity is a measure of the time scale of the problem. It also sets the time scale for a meaningful time-dependent simulation. Again, for low-injection velocity, it is necessary to provide an initial condition that includes an initial seed vortex, otherwise the simulation time becomes impractical.

Turbulence

Turbulence was modeled using the Jones-Launder/Sharma/Hanjalic (see Refs. 6–9 of Ref. 6) k-ε model with the wall treated as free slip; i.e., no boundary layer.

The SR experiment has a significant level of turbulence associated with the inlet flow. Because we do not know the inlet turbulence level, it is difficult to obtain a reasonable quantitative match to the experimental results. Given these limitations we tended to concentrate more on the scaling issues discussed previously, rather than attempting to match the experimental data. On the other hand, we did attempt to understand the impact of turbulence on the vortex formation and evolution.

A comparison between an inviscid and turbulent simulation is shown in Fig. 10. These simulations are for the baseline case. For reference, the experimental points are indicated. Relative to an inviscid simulation, the basic impact of turbulence

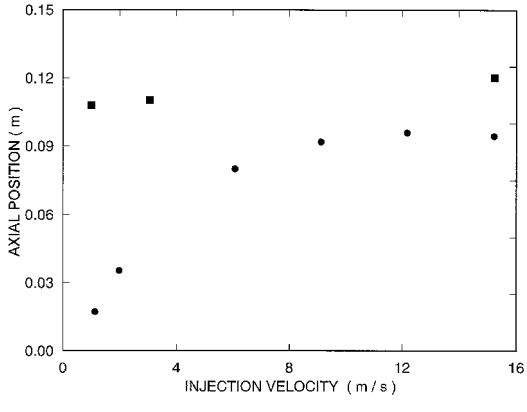

Fig. 9 Axial vortex position as a function of inlet injection velocity: ■, coarse mesh; ●, fine mesh.

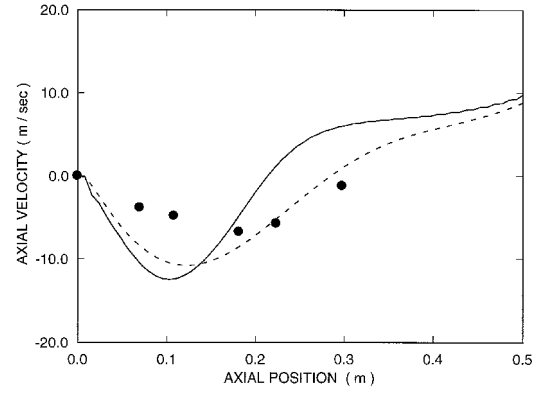

Fig. 10 Axial velocity as a function of axial position on the centerline, for an inviscid (——) and turbulent (– – –) flow. The SR experimental data points are indicated by ●. All parameters correspond to the baseline configuration.

is to move the average axial position of the vortex downstream, reduce the vorticity, and impose a small-scale, time-dependent motion on the vortex position. In the case shown the inlet turbulent energy is 1% of the inlet flow kinetic energy. At this level of inlet turbulence the agreement between the turbulent simulation and the experiment is not very good.

Although we do not know the turbulence level associated with the inlet flow, we have changed the level of inlet turbulence in an attempt to understand the impact of inlet turbulence on the vortex. The inlet turbulent kinetic energy has been varied from 1 to 10% of the inlet-flow kinetic energy. However, we do not observe a strong dependence of the position or size of the vortex on the inlet turbulence. At the very least these results lead us to question the validity of the axisymmetric assumption.

Long-Time Evolution and Stability

With a small amount of artificial viscosity applied over a specific region, very extensive simulations can be performed to investigate the long-time behavior of the vortex in the axisymmetric limit. For these simulations the geometry is identical to the SR experiment. We considered two injection velocities: low = 3 m/s, and high = 15.25 m/s. Both injection velocities produce a vortex whose dimensions are set by the geometry. For each case a coarse- and a fine-zone mesh was used. In addition, we considered both inviscid and turbulent flow models.

In the absence of large base-injection flow and with a nozzle the vortex appears to be stable with respect to shedding, disruption, and subsequent loss out of the nozzle. With a time-independent injection velocity and inviscid flow the vortex settles down to a fixed axial and radial position. If the injection velocity is then changed slightly the vortex will move. But again, the vortex settles down to fixed, but different, axial and radial position.

With a time-independent injection velocity and turbulent flow the axial and radial vortex position continue to move around. The motion is not periodic. The extent of the movement is about 10% the size of the vortex. Again, there is no evidence of shedding, disruption, and subsequent loss out of the nozzle, just jitter.

Again, it is important to understand that these stability results only apply to a two-dimensional axisymmetric configuration with a nozzle. In three dimensions, there are additional degrees of freedom that might allow a vortex to form but then disrupt or shed. This entire formation-disruption process would then repeat. Thus, at the very least, any new OCGCNR model should have the capability to investigate three-dimensional and time-dependent hydrodynamic flow.

Conclusions

The fundamental reason for the development of a more comprehensive OCGCNR model is to investigate more realistic configurations, all of which are three-dimensional in nature. Thus, in addition to gaining a qualitative understanding of the SR experiment, this scoping study was intended to determine what limitations exist within the most comprehensive axisymmetric OCGCNR model.

From the standpoint of computation, artificial viscosity has a significant impact on the simulation of a vortex. This problem is not severe with the high-injection velocity used in the SR experiment. However, a full-scale simulation will have an injection velocity of roughly two orders of magnitude lower than the SR experiment. Without a careful computational treatment, artificial viscosity can significantly distort the physical characteristics of the vortex or, even worse, prevent the formation of the vortex.

We find there is no inconsistency between a comprehensive axisymmetric full-scale engine simulation and the SR experiment. Rather, the presence or absence of a vortex depends upon the base-bleed injection ratio. This means that the full-scale engine simulation and the SR experiment are in different flow regimes.

The engine nozzle must be included in an OCGCNR model to correctly understand vortex formation and vortex stability. In making this statement we assume the engine will be as compact as possible to reduce the mass of the rocket. In addition, we infer that a self-consistent treatment of the nozzle will impact the uranium loss rate out the nozzle. Physically, the position of the vortex depends upon the inlet geometry, the inlet injection velocity, the nozzle position and geometry, the base-bleed injection ratio, and turbulence. The rotation rate associated with the vortex depends primarily upon injection velocity and turbulence.

In two-dimensional axisymmetric simulations with a nozzle the vortex appears to be stable with respect to disruption and subsequent loss out of the nozzle. However, the vortex can be disrupted and forced out the nozzle by a large base-bleed ratio. With a time-independent injection velocity and inviscid flow, the vortex appears to settle down to a fixed axial position. With a time-independent injection velocity and turbulent flow the axial and radial position of the vortex continues to move around. The size of the movement is less than 10% of the size of the vortex and the motion does not appear periodic.

The large discrepancy between the two-dimensional axisymmetric simulations and the three-dimensional experiment leads to the issue of a three-dimensional model. If the goal is to quantitatively match the SR experimental results, the simulation model needs to be three dimensional. The SR experiment appears to exhibit a stable recirculation region. Nevertheless, the experimental diagnostics are not time resolved. Under these conditions, a time-integrated formation-disruption process could appear to be a well-defined structure. In three dimensions, provided the vortex is stable with respect to disruption and shedding, the vortex may still move around. None of these issues can be resolved with a two-dimensional axisymmetric simulation; a three-dimensional simulation model will be required.

Acknowledgments

This research was funded by the Office of Advanced Space Technology, Marshall Space Flight Center, Contract H-28025, and the Department of Energy. The authors gratefully acknowledge informative discussions with B. DeVolder, R. Hotchkiss, D. Poston, P. Sforza, and D. Zerkle.

References

[1]Paine, T., *Pioneering the Space Frontier: The Report of the National Commission on Space*, Bantam Books, New York, 1986.

[2]Cohen, A., "Report of the 90-Day Study on Human Exploration of the Moon and Mars," NASA Internal Rept., Washington, DC, Nov. 20, 1989.

[3]Stafford, T. P., "America at the Threshold: Report of the Synthesis Group on America's Space Exploration Initiative," Superintendent of Documents, U.S. Government Printing Office, Washington, D.C., 1991.

[4]Poston, D. I., and Kammash T., "A Computational Model for an Open-Cycle Gas Core Nuclear Rocket," *Nuclear Science Engineering*, Vol. 122, No. 1, 1996, pp. 32–54.

[5]Sforza, P. M., Cresci, R. J., Arzt, J., and Castrogiovanni, A., "Recirculation Containment for Gas Core Fission Rockets," AIAA Paper 94-2899, June 1994.

[6]Cline, M. C., "VNAP2: A Computer Program for Computation of Two-Dimensional, Time-Dependent, Compressible, Turbulent Flow," Los Alamos National Lab. Rept. LA-8872, Los Alamos, NM, Aug. 1981.